J. Min. Metall. Sect. B-Metall. 54 (2) B (2018) 261 - 270

Journal of Mining and Metallurgy, Section B: Metallurgy

ACTIVITY AND DIFFUSIVITY OF OXYGEN IN THE LIQUID DILUTE Bi_xSb_{1-x} SOLUTIONS

D. Jendrzejczyk-Handzlik*, P. Handzlik, K. Fitzner

AGH University of Science and Technology, Faculty of Non-ferrous Metals, Krakow, Poland

(Received 11 March 2018; accepted 30 August 2018)

Abstract

The diffusivity and activity coefficient of oxygen in liquid antimony, bismuth and antimony-bismuth alloys were determined from coulometric titration experiments, which were performed in the temperature range from 985 to 1185 K. The diffusivity in pure metals (in cm2/s) is:

$$D_O^{Bi} = (9.04 \pm 1.82) \cdot 10^{-3} \exp\left(\frac{-49115 \pm 1809}{RT}\right)$$

$$D_O^{Sb} = (2.87 \pm 0.22) \cdot 10^{-4} \exp\left(\frac{-16720 \pm 677}{RT}\right)$$

The standard free energy of solution of oxygen in liquid antimony, bismuth and antimony-bismuth alloys according to the reaction ½ O_2 (g) = O (infinite dilution) is calculated. The activity coefficient of oxygen $\gamma^0_{O(Bi,\ Sb\ or\ Bi\text{-}Sb)}$ was calculated at 1085 K as a function of the alloy composition. It was demonstrated that Wagner's model with one adjustable parameter h gave a satisfactory description of the experimental data.

Keywords: *Coulometric titration method; Activity coefficient of oxygen; Diffusivity of oxygen; Bi-Sb alloys*

1. Introduction

Bismuth and antimony are semimetals which exhibit rhombohedral structure with similar lattice parameters. Binary bismuth-antimony phase diagram indicates complete solubility of these components in both the solid and liquid state. However, below the temperature of about 450 K, the miscibility gap in the solid state may appear. It is demonstrated on the calculated phase diagram [1] shown in Fig.1.

It was found that the substitution of Bi atoms by Sb atoms in this lattice modifies the band structure of bismuth. Bi-Sb alloys in the Bi-rich concentration region have a band structure similar to that of pure Bi. It is a semimetal in which the conduction and valence bands overlap at all temperatures. Addition of antimony results in the change of the overlap between bands and the alloy becomes a semiconductor with the energy gap increasing with increasing Sb concentration. What is interesting however, for Sb concentration above 40 % the band gap disappears again, and the semi-metallic character of the alloy returns [2,3]. This unusual behavior brings about a number of interesting transport properties of this alloy resulting from the dependence of the valence and conduction bands on alloy composition, temperature, external pressure and magnetic field. These effects were experimentally demonstrated by Smith and Wolfe [4], who showed that Bi-rich alloys have higher figures of merit (i.e. the ratio of squared Seebeck coefficient divided by the product of the thermal conductivity and electrical resistivity, which determines the usefulness of the material in thermoelectric applications) than those obtained for Bi_2Te_3 in the temperature range 20–220 K. Later Cuff et al. [5], demonstrated that this effect can be enhanced by the application of transverse magnetic

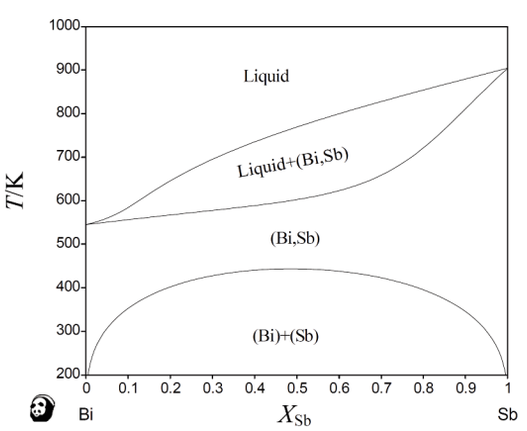

Figure 1. *Bi-Sb phase diagram [1].*

**Corresponding author: djendrze@agh.edu.pl*

DOI:10.2298/JMMB180311014J

field, which proved that Bi-Sb alloys can be used in solid-state cooling devices. Yim and Amith [6] investigated thermoelectric and thermomagnetic properties of un-doped Bi–Sb homogeneous single crystals as a function of temperature, magnetic field and crystallographic direction. Obtained thermoelectric and thermomagnetic properties indicate that Bi-Sb mixed crystals together with Bi_2Te_3 are the best cooling materials found to date [7]. It is confirmed by the recent study of Luo et al. [8], Malik et al. [9] and Combe et al. [10] which demonstrated that the method of the alloys preparation can significantly improve their thermoelectric properties.

Moreover, recent advances in condensed matter physics leading to the discovery of topological insulators, made Bi-Sb alloys an object of angle-resolved photoemission spectroscopy (ARPES) investigations, since 3D topological insulator was predicted in the Bi_xSb_{1-x} alloy within a certain range of composition [11]. Boltasseva and Atwater [12] mentioned Bi-Sb system as the potential candidate among various alloys for metamaterials applications. Thus, seemingly simple Bi-Sb solid solution can exhibit a large variety of interesting thermophysical properties being fitted for various applications.

However, the study of physical properties requires high-quality materials which are usually single crystals [13]. The process to prepare them is not so simple because due to the very low diffusion rates in the solid state and the character of the phase diagram the resulting crystal suffers from large segregation. The solution of the problem is either to maintain constant composition of the melt during the growth, or to use the process of homogenization. In both cases the contact with the surrounding atmosphere is unavoidable. Severe requirements regarding purity of crystals during growth from the liquid phase cause a need for the data on thermodynamics of solutions containing potential inclusions like oxygen dissolved in liquid metals. Both bismuth and antimony form thermodynamically not very stable sesquioxides and consequently, the saturation solubility of oxygen in these metals is relatively high [14]. Recently, another good reason to study these solutions emerged due to the development of high power heat transport systems. Hosemann et al. [15] mentioned both Bi and Sb as possible elements for liquid metal in cooled power systems, where in loop systems high temperature corrosion can be controlled depending on oxygen activity. Thus, there is a question about equilibrium oxygen pressure one must fix in the surrounding atmosphere to remove oxygen from the metal. Moreover, the study of the oxygen activity in dilute solutions can be considered as the first step in the investigations of the ternary Bi-Sb-O system. Several solid phases were found to exist in this system [16] but their thermodynamic stability as well as phase relations remain unknown.

Literature review indicates that oxygen activity in dilute Bi-Sb solutions was measured only once by Otsuka et al. [17]. No diffusion data on oxygen in these solutions were reported so far.

To derive required properties an electrochemical method was used. There is a very precise method based on solid oxide galvanic cells called coulometric titration which can be used for gathering experimental data on oxygen behavior in liquid metals and their alloys. This method, implemented first time by Alcock and Belford [18,19] to the study of oxygen solubility in liquid lead and tin, is used in the present work. Its big advantage is in the fact that both activity and diffusivity of oxygen in the alloy can be derived from the same experiment.

2. Experimental

Metallic bismuth and antimony used in this study were 99.99 mass.% pure and were obtained from Sigma Aldrich, Germany. The fully stabilized ZrO_2+Y_2O_3 (YSZ) electrolyte tubes, closed at one end YSZ electrolyte tubes (length 400 mm, outside diameter 8 mm), were supplied by Yamari, Japan. The iridium, tungsten, rhenium and platinum wires (diameter 0.5 mm) were 99.99 mass.% obtained from Alfa Aesar, Germany (Ir, Re, W) and from the Polish Mint, Poland (Pt), respectively. The Kanthal™ wire was obtained from Kanthal AB, Sweden. Argon gas flowing through the cell was obtained from Air Products and was 99.99 mass.% pure.

The arrangement of the electrochemical cell:

$$\underline{O} \text{ in } Bi_xSb_{1-x}/ZrO_2+Y_2O_3/\text{ air} \qquad (1)$$

is shown in Fig.2. The solid electrolyte tube was placed in a vertical resistant furnace in such a manner that the cell was kept entirely within a constant temperature zone. The furnace tube was flushed with air from the outside, while a glass-head closing the electrolyte tube enabled circulation of purified argon within the tube. The electrical circuit consisted of two arts working independently. The circuit 1 was devoted to emf measurements at equilibrium state which yield equilibrium oxygen partial pressure. The circuit 2 was used to adjust the applied voltage *E* as well as to record the electrical current and number of coulombs passed. The emf of the cell and *E* applied were measured by means of a Keithley 2000 multimeter (Keithley Instruments, Inc., USA). *E* applied was adjusted by a potentiostat CHI 600C Series (CHI Instruments, Inc., USA), which also automatically recorded the current and the charge flowing through the cell. The course of the experiment was under control of a computer which was connected to the potentiostat and executed the acquisition software.

Argon gas was purified by passing over copper failings at 723 K. Before each experiment the electrolyte tube was flushed by purified argon via an H-shape tube for 10-12 h and then the furnace was slowly heated to the desired temperatures.

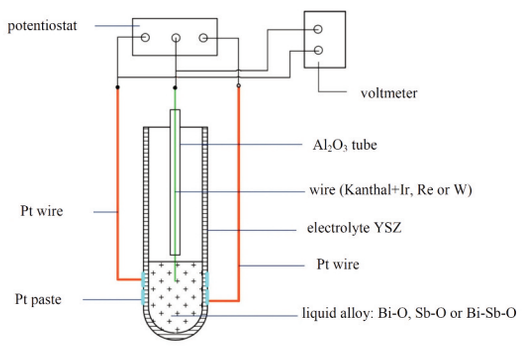

Figure 2. *Diagram of the electrochemical cell for coulometric titration experiments.*

After the required temperature had been reached, the cell was left for several hours to attain the equilibrium. Then, the equilibrium emf E_1 was measured by circuit 1. Next, the difference in voltage DE was applied to the cell by the circuit 2. This difference equaled 100-200 mV. The current flowing in the circuit 2 was recorded until the steady state was attained. However, the current never vanished completely at the steady state since the electronic current does pass through the electrolyte. Consequently, the measured current was corrected by subtracting electronic current I_e, which value can be obtained from the experimental I vs. time curves. In the meantime the quantity of electricity passed during experiment was recorded. Finally, the value of the emf at the steady state E_2 was measured by the circuit 1.

3. Results and discussion

Emf values produced by the cell (I) were corrected by thermo-emf's (Pt–Re+kanthal, Pt-Ir+kanthal and Pt-W+kanthal, respectively, using previously determined (E_{Re}=-0.2363-5,458´10^{-3}T+1,41´10^{-5}T^2 (mV), E_{Ir}=-2.3636´10^{-4}-5.458´10^{-7}T+8.32´10^{-9}T^2 (mV) and E_W=-0.2363-5.458´10^{-4}T+8.32´10^{-6}T^2 (mV)) functions [17].

The quantity of the electrical charge contributed by corrected I_{ion} was calculated by integrating the remaining current over time. Titration experiments were carried out four times at constant temperature, and then the temperature was changed and the whole procedure was repeated.

A typical I vs. time curve obtained during the potentiostatic experiment is shown in Fig. 3. Experiments were run for alloys of variable composition from pure bismuth to pure antimony, and in the temperature range from 985 to 1185 K. The obtained experimental results are gathered in Table 1.

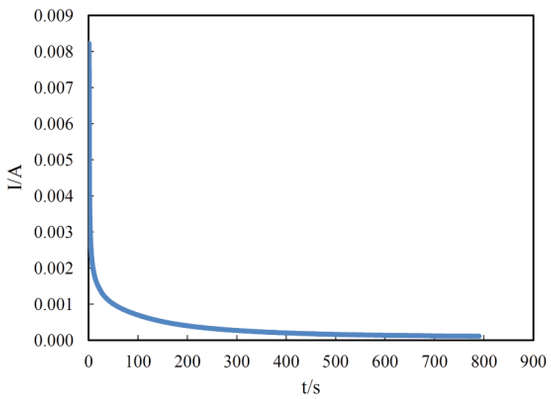

Figure 3. *Ionic current as a function of time, liquid antimony at 1085 K.*

Activity coefficients of oxygen in liquid alloy were calculated from the relation:

$$f^0_{O(Me)} = p^{\frac{1}{2}}_{O_2} / C_O(1) \quad (1)$$

where p_{O_2} is directly related to the measured emf through the equation:

$$E_1 = \frac{RT}{2F}\ln\left(\frac{0.21}{p^{1/2}_{O_2}}\right) \quad (2)$$

and the oxygen concentration can be obtained by solving the following two equations:

$$C_O(1) - C_O(2) = 100\frac{M}{W}\frac{\theta_{ion}}{2F} \quad (3)$$

and (assuming Henry's Law to be valid):

$$E_2 - E_1 = \Delta E = \frac{RT}{2F}\ln\left(\frac{C_O(1)}{C_O(2)}\right) \quad (4)$$

DE is an imposed potential difference, M is the atomic weight of the metal, W is the weight of liquid metal, θ_{ion} is the quantity of electricity passed due to ionic current and the oxygen concentration C_O is expressed in atomic percent.

The Gibbs free energy change of the reaction:

$$\tfrac{1}{2}\,O_2(g) = \underline{O}_{\text{alloy}} \quad (5)$$

can be expressed by the oxygen activity coefficient $f^0_{O(Me)}$:

$$\Delta G^0_{O(Me)} = RT\ln f^0_{O(Me)} = RT\ln\frac{p^{1/2}_{O_2}}{C_O} \quad (6)$$

The standard state for dissolved oxygen is an infinitely dilute solution in which the activity is equal to the concentration in atomic percent.

Equilibrium oxygen partial pressure and oxygen concentration can be calculated from measured emf's and the quantity of electricity passed due to I_{ion}. The values of $\Delta G^0_{O(Me)}$ obtained during experiments are shown in Fig. 4 as a function of temperature and alloy

Table 1. *Experimental values for liquid Bi, Sb and Bi-Sb alloys (E_1 and E_2 after thermo-emf correction).*

Run No.	T/K	E_1/V	E_2/V	C_1(O) at%	$\ln f^0_{O(Me)}$	Av. $\ln f^0_{O(Me)}(\pm\sigma)$	$\Delta G^0_{O(Me)}$ (J·mol^{-1})	Av. $\Delta G^0_{O(Me)}(\pm\sigma)$ (J·mol^{-1})
Bi, electric contact is kanthal+Ir								
1	1035	0.654	0.845	0.006668	-10.43	-10.28(±0.22)	-89750	-88425(±1787)
2	1035	0.639	0.829	0.006874	-10.12		-87082	
3	1035	0.637	0.830	0.008111	-10.24		-88115	
4	1035	0.635	0.830	0.006818	-10.03		-86308	
5	1035	0.681	0.874	0.004169	-10.56		-90869	
1	1085	0.702	0.886	0.002612	-9.84	-9.75(±0.12)	-88764	-87952(±1115)
2	1085	0.653	0.829	0.007510	-9.85		-88854	
3	1085	0.677	0.862	0.004186	-9.78		-88222	
4	1085	0.665	0.856	0.004402	-9.57		-86328	
5	1085	0.673	0.857	0.004866	-9.84		-88764	
6	1085	0.665	0.851	0.004597	-9.62		-86779	
1	1110	0.665	0.824	0.006281	-9.61	-9.49(±0.15)	-88686	-87599(±1383)
2	1110	0.660	0.819	0.005197	-9.31		-85918	
3	1110	0.644	0.809	0.008065	-9.42		-86933	
4	1110	0.721	0.875	0.001627	-9.43		-87025	
5	1110	0.655	0.844	0.007546	-9.58		-88409	
6	1110	0.657	0.837	0.007415	-9.61		-88686	
7	1110	0.653	0.853	0.006419	-9.38		-86564	
8	1110	0.700	0.865	0.003466	-9.75		-89978	
9	1110	0.605	0.807	0.016869	-9.34		-86195	
1	1135	0.668	0.820	0.006447	-9.39	-9.30(±0.05)	-88608	-87740(±488)
2	1135	0.683	0.838	0.004213	-9.27		-87475	
3	1135	0.680	0.852	0.004515	-9.28		-87570	
4	1135	0.690	0.842	0.003693	-9.28		-87570	
5	1135	0.651	0.841	0.008131	-9.27		-87475	
1	1160	0.668	0.800	0.005738	-8.98	-9.01(±0.11)	-86605	-86879(±1105)
2	1160	0.685	0.800	0.004124	-8.99		-86702	
3	1160	0.672	0.853	0.005236	-8.97		-86509	
4	1160	0.638	0.780	0.011036	-9.03		-87087	
5	1160	0.627	0.818	0.013841	-9.04		-87184	
6	1160	0.638	0.828	0.011149	-9.04		-87184	
1	1185	0.675	0.844	0.005450	-8.78	-8.85(±0.07)	-86501	-87158(±692)
2	1185	0.657	0.836	0.008862	-8.92		-87881	
3	1185	0.627	0.811	0.014734	-8.84		-87092	
Bi80Sb20, electric contact is kanthal+Ir								
1	1035	0.82	1.007	0.000464	-11.49	-11.48(±0.12)	-98871	-98785(±998)
2	1035	0.828	0.996	0.000389	-11.49		-98871	
3	1035	0.808	0.986	0.000596	-11.47		-98699	
4	1035	0.800	0.943	0.000716	-11.47		-98699	
1	1085	0.810	1.004	0.000698	-10.83	-10.85(±0.09)	-97694	-97874(±797)
2	1085	0.799	0.984	0.000890	-10.84		-97784	
3	1085	0.804	0.935	0.000808	-10.85		-97874	
4	1085	0.829	0.995	0.000488	-10.88		-98145	
1	1135	0.792	0.936	0.001254	-10.29	-10.29(±0.12)	-97100	-97077(±1091)
2	1135	0.796	0.943	0.001152	-10.28		-97006	
3	1135	0.800	0.994	0.001057	-10.28		-97006	
4	1135	0.790	0.986	0.001321	-10.30		-97195	
1	1185	0.781	0.901	0.001857	-9.78	-9.78(±0.11)	-96353	-96304(±1053)

The table continues on the next page

Table continuous from the previous page

2	1185	0.781	0.911	0.001825	-9.76		-96156	
3	1185	0.791	0.901	0.001518	-9.78		-96353	
4	1185	0.786	0.985	0.001676	-9.78		-96353	
Bi60Sb40, electric contact is kanthal+Ir								
1	1035	0.814	0.989	0.000810	-11.91	-11.91(±0.01)	-102485	-102507(±50)
2	1035	0.832	0.993	0.000555	-11.93		-102658	
3	1035	0.791	0.978	0.001325	-11.89		-102313	
4	1035	0.799	0.956	0.001150	-11.92		-102571	
1	1085	0.800	0.985	0.001360	-11.29	-11.28(±0.02)	-101844	-101776(±147)
2	1085	0.801	0.981	0.001317	-11.28		-101753	
3	1085	0.795	0.936	0.001511	-11.28		-101753	
4	1085	0.828	1.002	0.000744	-11.28		-101753	
1	1135	0.789	0.924	0.001897	-10.64	-10.65(±0.01)	-100403	-100521(±90)
2	1135	0.786	0.933	0.002061	-10.66		-100592	
3	1135	0.745	0.974	0.004756	-10.66		-100592	
4	1135	0.776	0.976	0.002509	-10.65		-100498	
1	1185	0.770	0.890	0.003189	-10.11	-10.11(±0.01)	-99605	-99629(±95)
2	1185	0.791	0.921	0.002144	-10.12		-99703	
3	1185	0.762	0.889	0.003766	-10.12		-99703	
4	1185	0.792	0.996	0.002066	-10.1		-99506	
Bi50Sb50, electric contact is kanthal+Re								
1	1035	0.771	0.972	0.003174	-12.31	-12.27(±0.08)	-105927	-105583(±699)
2	1035	0.745	0.945	0.004789	-12.14		-104465	
3	1035	0.739	0.938	0.006417	-12.30		-105841	
4	1035	0.752	0.948	0.004946	-12.33		-106100	
1	1085	0.724	0.889	0.009995	-11.66	-11.56(±0.11)	-105181	-104279(±952)
2	1085	0.777	0.899	0.002624	-11.45		-103287	
3	1085	0.748	0.883	0.005907	-11.64		-105001	
4	1085	0.742	0.870	0.005751	-11.49		-103648	
1	1135	0.729	0.817	0.009337	-11.01	-10.93(±0.11)	-103895	-103093(±1041)
2	1135	0.701	0.813	0.014057	-10.84		-102290	
3	1135	0.780	0.893	0.003368	-11.03		-104083	
4	1135	0.762	0.952	0.003944	-10.82		-102102	
1	1185	0.703	0.824	0.017886	-10.52	-10.40(±0.13)	-103644	-102486(±1280)
2	1185	0.713	0.831	0.011640	-10.29		-101378	
3	1185	0.704	0.837	0.017442	-10.51		-103545	
4	1185	0.694	0.880	0.017042	-10.29		-101378	
Bi40Sb60, electric contact is kanthal+Re								
1	1035	0.771	0.972	0.005986	-12.94	-12.95(±0.12)	-111349	-111414(±1014)
2	1035	0.777	0.978	0.005351	-12.97		-111607	
3	1035	0.762	0.958	0.007297	-12.94		-111349	
4	1035	0.787	0.993	0.004160	-12.94		-111349	
1	1085	0.800	0.869	0.003312	-12.18	-12.19(±0.08)	-109872	-109962(±731)
2	1085	0.762	0.866	0.007642	-12.20		-110052	
3	1085	0.797	0.859	0.003564	-12.19		-109962	
4	1085	0.778	0.926	0.005383	-12.19		-109962	
1	1135	0.769	0.917	0.007178	-11.56	-11.59(±0.14)	-109085	-109368(±1326)
2	1135	0.775	0.889	0.006782	-11.63		-109745	
3	1135	0.753	0.876	0.010737	-11.64		-109840	
4	1135	0.760	0.894	0.008349	-11.53		-108802	
1	1185	0.677	0.826	0.051537	-11.07	-11.02(±0.10)	-109063	-108521(±946)

The table continues on the next page

Table continuous from the previous page

2	1185	0.736	0.879	0.015949	-11.05		-108866	
3	1185	0.756	0.897	0.010145	-10.99		-108274	
4	1185	0.798	0.932	0.004292	-10.95		-107880	
Bi20Sb80, electric contact is kanthal+Re								
1	1035	0.771	0.972	0.007890	-13.22	-13.21(±0.04)	-113758	-113694(±333)
2	1035	0.775	0.975	0.007095	-13.20		-113586	
3	1035	0.769	0.97	0.008253	-13.22		-113758	
4	1035	0.772	0.973	0.007618	-13.21		-113672	
1	1085	0.782	0.944	0.006398	-12.45	-12.45(±0.18)	-112308	-112263(±1623)
2	1085	0.803	0.962	0.005101	-12.67		-114292	
3	1085	0.730	0.879	0.015625	-12.23		-110323	
4	1085	0.779	0.979	0.006708	-12.43		-112127	
1	1135	0.769	0.931	0.008623	-11.75	-11.8(±0.10)	-110878	-111373(±957)
2	1135	0.774	0.973	0.008662	-11.85		-111821	
3	1135	0.773	0.931	0.008655	-11.83		-111632	
4	1135	0.762	0.919	0.010339	-11.78		-111161	
1	1185	0.705	0.865	0.034674	-11.22	-11.23(±0.07)	-110540	-110590(±661)
2	1185	0.753	0.910	0.013857	-11.24		-110737	
3	1185	0.755	0.896	0.012867	-11.21		-110442	
4	1185	0.757	0.915	0.012586	-11.23		-110639	
Sb, electric contact is kanthal+W								
1	985	0.828	1.010	0.001166	-14.19	-14.19(±0.02)	-116206	-116239(±180)
2	985	0.849	1.031	0.001093	-14.20		-116288	
3	985	0.910	1.098	0.000336	-14.22		-116452	
4	985	0.833	1.023	0.000968	-14.20		-116288	
5	985	0.824	1.013	0.001203	-14.16		-115960	
1	1035	0.884	1.065	0.000579	-13.14	-13.38(±0.12)	-113070	-115092(±1000)
2	1035	0.833	1.013	0.001529	-13.44		-115651	
3	1035	0.810	0.993	0.002120	-13.40		-115307	
4	1035	0.815	0.999	0.001920	-13.42		-115479	
5	1035	0.808	0.992	0.002602	-13.41		-115393	
6	1035	0.810	0.994	0.002230	-13.44		-115651	
1	1085	0.833	1.009	0.001985	-12.65	-12.65(±0.02)	-114112	-114135(±113)
2	1085	0.825	1.007	0.002356	-12.67		-114292	
3	1085	0.822	1.008	0.002513	-12.65		-114112	
4	1085	0.813	0.997	0.002919	-12.64		-114022	
1	1135	0.839	1.016	0.002314	-11.94	-11.94(±0.02)	-112670	-112651(±182)
2	1135	0.826	1.018	0.002688	-11.93		-112576	
3	1135	0.801	0.987	0.004352	-11.95		-112765	
4	1135	0.805	1.000	0.003883	-11.91		-112387	
5	1135	0.806	0.998	0.003905	-11.96		-112859	
1	1185	0.791	0.975	0.006246	-11.37	-11.36(±0.02)	-112018	-111920(±156)
2	1185	0.792	0.979	0.006001	-11.35		-111821	
3	1185	0.788	0.968	0.006047	-11.36		-111920	
4	1185	0.800	0.985	0.005096	-11.38		-112117	
5	1185	0.791	0.979	0.005722	-11.34		-111723	

compositin. They are also gathered in the form of equations in Table 2 together with standard error of linear regression which represent the uncertainty of our results.

The variation of $\ln f^{0}_{O(Me)}$ vs. alloy composition at the chosen temperature 1085 K is shown in the next Fig. 5a. It is seen that this composition dependence is mainly generated by the end-points, i.e. the difference between logarithms of the activity coefficient of oxygen being at infinite dilution in pure bismuth and pure antimony.

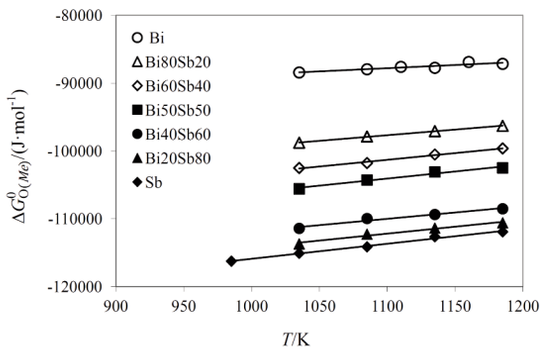

Figure 4. *Free energy of oxygen dissolution in liquid Bi, Sb and Bi-Sb alloys.*

Table 2. *The values of $\Delta G^0_{O(Me)}$ obtained during experiment as a function of temperature and Bi-Sb alloys composition (S is standard error of linear regression)*

X_{Sb}	$\Delta G^0_{O(Me)}$ /(J·mol^{-1})	S/(J·mol^{-1})
0	9.439T-98181	±1305
0.2	16.480T-115803	±1145
0.4	19.778T-123062	±1700
0.5	20.954T-127119	±1190
0.6	18.546T-130402	±1207
0.8	20.404T-134628	±1185
1	22.156T-138047	±5470

In order to describe oxygen activity coefficients $\gamma^0_{O(Me)}$ the binary Bi-Sb alloy we used Wagner's model [18]. Since deviation of this alloy from ideality is not large [1], one may assume that distribution of solvent atoms in this alloy is close to random. This is one of Wagner's basic assumptions. The dissolution of oxygen is expressed as transfer of oxygen from the gas phase on a vacant quasi-interstitials side surrounded by the solvation shell containing z=6 metal atoms.

The original Wagner's equation has the form:

$$\gamma^0_{O(Me)} = \left(\sum_{i=0}^{i=z} \frac{z!}{i!(z-i)!} \left(\frac{1-X_{Bi}}{\gamma^0_{O(Sb)}^{\frac{1}{z}}} \right)^{z-i} \left(\frac{X_{Bi}}{\gamma^0_{O(Bi)}^{\frac{1}{z}}} \right)^{i} \cdot \exp\left(\frac{(z-i)ih}{2RT} \right) \right)^{-1} \quad (7)$$

where h is a constant energy parameter which is adjustable. In Eq. (7) concentrations of alloy components are expressed in mole fractions. It requires the change of the standard state at infinite dilution from atomic percent to oxygen mole fraction. Consequently, our experimental results can be easily recalculated changing oxygen concentration at.%/100=X_O and activity coefficient $\gamma^0_O = f^0_O \cdot 100$.

The fitting procedure was performed with MathCad15 software. Calculated and experimental results are shown and compared in Figs. 5a and 5b. As can be seen from Fig. 5b the calculation performed with h=841 (J×mol^{-1}) gave a satisfactory representation of the data obtained in the present work.

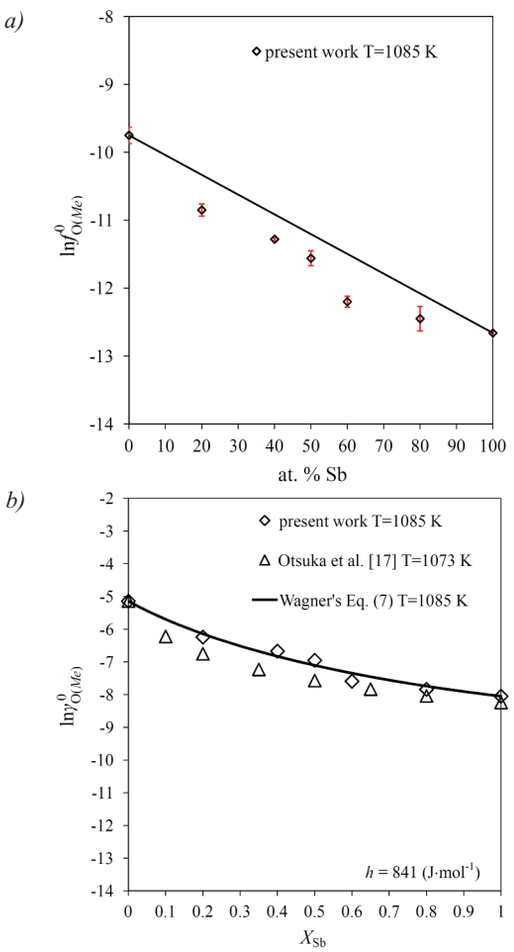

Figure 5. *Variation of $\ln f^0_{O(Me)}$ at 1085 K with: a) at. % of antimony; b) mole fraction of antimony*

In order to obtain D^{Me}_O from the experimental data, the solution of Fick's second Law for cylindrical coordinates:

$$\frac{\partial C_O}{\partial t} = \left(\frac{1}{r} \right) \left(rD^{Me}_O \left(\frac{\partial C_O}{\partial r} \right) \right) \quad (8)$$

given by Crank [22] and implemented by Ramanarayanan and Rapp [23] as well as Oberg et al. [24] is used. After necessary rearrangements one arrives at its final form:

$$I_{ion} = 8\pi aFD^{Me}_O \left[C_O(1) - C_O(2) \right] \exp\left(\frac{-2.405^2 D^{Me}_O t}{r^2} \right) \quad (9)$$

where I_{ion} represents ionic current determined experimentally, C_O represents the oxygen concentration in the metal in mol/cm^3, D^{Me}_O is the diffusion coefficient of oxygen in metal in cm^2/s, t is time in s, r is the radius of the electrolyte tube in cm, a is the height of the liquid metal column and the

constant 2.405 is the first root of the Bessel function of zero order.

The logarithm of Eq. (9) yields the linear dependence:

$$\ln I_{ion} = A - Bt \tag{10}$$

and from the value of B the diffusion coefficient D_O^{Me} can be obtained. In the construction of $\ln I_{ion}$ vs. time dependencies, the results obtained for time shorter than 5–10 minutes were usually discarded, and were not taken into account during calculations. Having the dependence (10) established for each alloy composition, in this way $\ln D_O^{Me}$ vs. $1/T$ plots for fixed alloy composition were calculated and are gathered in Table 3.

In Fig. 6a the diffusion coefficient of oxygen in liquid bismuth and antimony as a function of temperature is shown. Results obtained in the present work are compared with the literature data published by Fitzner [25, 26]. Values obtained in the present work are described by following equations:

$$D_O^{Bi} = (9.04 \pm 1.82) \cdot 10^{-3} \exp\left(\frac{-49115 \pm 1809}{RT}\right) \tag{11}$$

$$D_O^{Sb} = (2.87 \pm 0.22) \cdot 10^{-4} \exp\left(\frac{-16720 \pm 677}{RT}\right) \tag{12}$$

which give the temperature dependence of oxygen diffusion coefficients. Activation energies are expressed in J×mol^{-1}. Due to small set of the experimental data, the uncertainty was estimated by using conservative "two sigma" estimator. It is assumed that similar uncertainty must correspond to oxygen diffusion coefficients in alloys.

The comparison of the literature data with those from the present work showed that and $\ln D_O^{Bi}$ obtained $\ln D_O^{Bi}$ in the present work are a little lower than those taken from the literature. However, this difference is maximum 3%, so they are in good agreement.

In Fig. 6b the variation of $\ln D_O$ in Bi-Sb alloys is shown at the chosen temperature 1185 K. It is seen that diffusion slows down around X_{Sb}=0.2. It is the composition which corresponds to the change in electronic structure in the solid alloy. It may indicate the change in transport mechanism.

Table 3. *Results of coulometric titration experiments performed on liquid Bi-O, Sb-O and Bi-Sb-O solutions.*

T/K	$lnI_{ion}=A-Bt$		r/cm	a/cm
	A	B		
Bi				
985	13.23651	0.00107	0.4	2.5
1035	8.76231	0.00139		
1085	2.1523	0.00182		
1135	10.12861	0.00238		
1185	3.92512	0.00291		
Bi80Sb20				
1185	8.19178	0.00178	0.35	2.6
Bi60Sb40				
1185	5.08472	0.00183	0.35	2.4
Bi50Sb50				
1185	6.77998	0.00188	0.35	2.55
Bi40Sb60				
1185	4.39157	0.00197	0.35	2.48
Bi20Sb80				
1185	5.0972	0.00238	0.35	2.36
Sb				
985	7.4042	0.00175	0.4	2.5
1035	2.54052	0.00196		
1085	2.1523	0.00212		
1135	10.12861	0.00231		
1185	3.92512	0.00249		

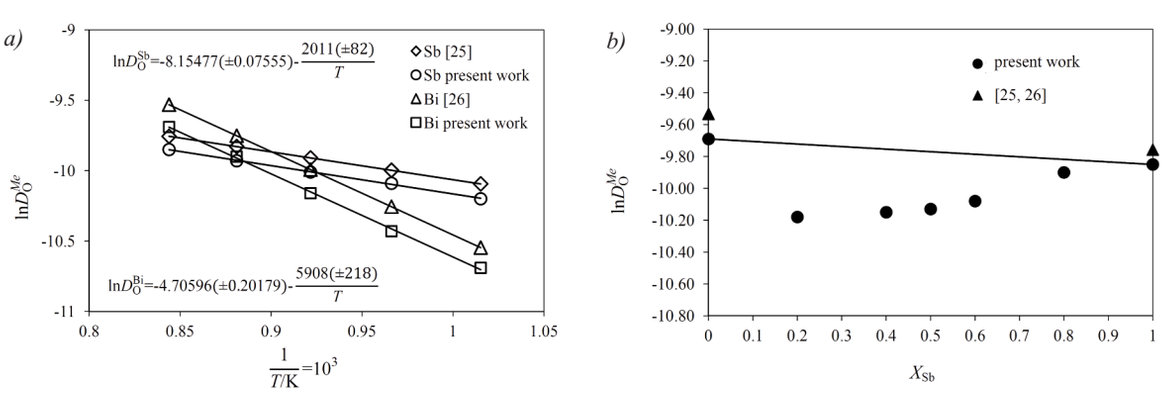

Figure 6. *The diffusion coefficient of oxygen in liquid antimony and bismuth: a) as a function of temperature; b) at 1185 K.*

Summarizing, activity coefficient of oxygen in liquid antimony, bismuth and antimony-bismuth alloys were determined from coulometric titration experiments which were performed in the temperature range from 985 to 1185 K. The results obtained for the free energy change of the reaction of dissolution (5) in pure liquid antimony and bismuth were compared with the literature data of Fitzner [25, 26] and Otsuka et al. [17] and Otsuka and Kozuka [27]. They applied the same experimental method as that used in the present work, and the comparison of the obtained results gave very good agreement. The difference between them and the results of the present work is about 2%. Similarly, the comparison of the results obtained for free energy change of the reaction (5) in Bi-Sb alloys with the data of Otsuka et al. [17] shows good agreement too. It is demonstrated in Fig. 5b, where $\ln\gamma^0_{O(Me)}$ values are compared for different alloy compositions.

Results obtained in the present work were described with Wagner's model to calculate the as a function of the alloy composition. Calculations were performed at chosen temperature 1085 K. As can be seen from Fig. 5b, the calculations performed with parameter h=841 (J×mol^{-1}) gave a satisfactory representation of the data obtained in the present work. Next, the obtained results were compared with the data of Otsuka et al. [17] determined at 1073K. The maximum difference between them is 8%, and it indicates good agreement. As one can see all the results of $\ln\gamma^0_{O(Me)}$ in Bi-Sb system are consistent.

Finally, the diffusion coefficients of oxygen in liquid antimony, bismuth and antimony-bismuth alloys were determined. Diffusion coefficients D_O^{Bi} and D_O^{Sb} determined in the present work are described by Eqs. (11) and (12). The obtained results are compared with the literature data [25, 26] and again they show good agreement. However, their temperature dependence revealed that oxygen behaves differently in bismuth and antimony. At lower temperature oxygen diffusion is faster in antimony and then, with the increasing temperature, it becomes faster in bismuth. This behavior is shown in Fig. 6a. The dependence of the logarithm of oxygen diffusion coefficient with the alloy concentration is not linear. It shows deviation from linear dependence (Fig. 6b), with the minimum located at approximately X_{Sb}=0.2 i.e. at the composition for which the alloy becomes a semiconductor. There is no theory which can explain this kind of behavior. It is worth mentioning that the results of oxygen diffusion in the Bi-Sb alloys were obtained for the first time.

4. Conclusions

In this work, coulometric titration experiments were used to determine Gibbs free energy of oxygen dissolution in liquid Bi, Sb and Bi-Sb alloys in the temperature range from 985 to 1185 K. Variation of $\ln\gamma^0_{O(Me)}$ with the alloy composition is not linear. It was found that this dependence can be described with Wagner's model with one constant parameter h=841 (J×mol^{-1}). From the same experiment diffusion coefficients of oxygen in liquid Bi, Sb and Bi-Sb alloys were determined. Again, the dependence of $\ln D_O$ on alloy composition is not linear, with the minimum around 0.2 mole fraction of antimony. There is no theory however, which can explain this type of behaviour.

Acknowledgements

This work was supported by the Polish Ministry of Science and Higher Education at AGH University of Science and Technology, Faculty of Non-Ferrous Metals under grant No IP2012 0442 72.

References

[1] A. Kroupa, A.T. Dinsdale, A. Watson, J. Vrestal, J. Vizdal, A. Zemanova, COST 531 database v.3.0, 2008

[2] A.L. Jain, Physical Review Journals, 114(6) (1959) 1518-1528.

[3] B. Lenoir, M. Cassart, J. -P. Michenaud, H. Scherrer, S. Scherrer, Journal of Physics and Chemistry of Solids, 57(1) (1996) 89-99.

[4] G.E. Smith, R. Wolfe, Journal of Applied Physics, 33(3) (1962) 841-846.

[5] K.F. Cuff, R.B. Horst, J.L. Weaver, S.R. Hawkins, C.F. Kooi and G.M. Enslow, Applied Physics Letters, 2(8) (1963) 145-146.

[6] W.M. Yim, A. Amith, Solid-State Electronics, 15(10) (1972) 1141-1165.

[7] G.A. Slack, New Materials and Performance Limits for Thermoelectric Cooling, CRC Handbook of Thermoelectrics, (ed. D. M. Rowe), CRC Press, Boca Raton, 1995, 407-440.

[8] T. Luo, S. Wang, H. Li, X. Tang, Intermetallics, 32 (2013) 96-102.

[9] K. Malik, D. Das, S.K. Neogi, A.K. Deb, A. Dasgupta, S. Bandyopadhyay, A. Banerjee, Journal of Physics and Chemistry of Solids, 91 (2016) 7–12.

[10] E. Combe, R. Funahashi, T. Takeuchi, T. Barbier, K. Yubuta, Journal of Alloys and Compounds, 692 (2017) 563-568.

[11] X.-L. Qi, S.-C. Zhang, Reviews of Modern Physics, 83(4) (2011) 1057-1110.

[12] A Boltasseva, H.A. Atwater, Science, 331(6015) (2011) 290-291.

[13] D. Hsieh, D. Qian, L. Wray, Y. Xia, Y.S. Hor, R.J. Cava, M.Z. Hasan, Nature, 452(7190) (2008) 970-974.

[14] Y.A. Chang, K. Fitzner, M.-X. Zhang, Progress in Materials Science, 32(2-3) (1988) 97-259.

[15] P. Hosemann, Liquid metal coolants for high power heat transport systems, MatISSE/JPNM workshop, November 25th, 2015.

[16] A. Tairi, J.-C. Champarnaud-Mesjard, D. Mercurio, B. Frit, Revue De Chimie Minérale, 22 (1985) 699-710.

[17] S. Otsuka, Y. Kurose, Z. Kozuka, Metallurgical Transactions B, 15B (1984) 141-147.
[18] C.B. Alcock, T.N. Belford, Transactions of the Faraday Society, 60 (1964) 822-835.
[19] T.N. Belford, C.B. Alcock, Transactions of the Faraday Society, 61 (1965) 443-453.
[20] B. Onderka, Ph.D. Thesis, IMIM PAN, Krakow, 1994.
[21] C. Wagner, Acta Metallurgica, 2 (1973) 1297-1303.
[22] J. Crank, The Mathematics of Diffusion, 2nd Ed., Oxford Univ. Press, Oxford, 1975.
[23] T. A. Ramanarayanan, R.A. Rapp, Metallurgical Transactions, 3(12) (1972) 3239-3246.
[24] K.E. Oberg, L.W. Friedman, W.M. Boorstein, R.A. Rapp, Metallurgical Transactions, 4(1) (1973) 61-67.
[25] K. Fitzner, Zeitschrift fur Metallkunde, 71 (1980) 178-181.
[26] K. Fitzner, Thermochimica Acta, 35 (1980) 277-286.
[27] S. Otsuka, Z. Kozuka, Metallurgical Transactions B, 10 (1979) 565-574.

AKTIVNOST I DIFUZIVNOST KISEONIKA U TEČNIM RAZBLAŽENIM Bi_xSb_{1-x} RASTVORIMA

D. Jendrzejczyk-Handzlik*, P. Handzlik, K. Fitzner

AGH univerzitet nauke i tehnologije, Fakultet za obojene metale, Krakov, Poljska

Apstrakt

Koeficijent difuzivnosti i aktivnosti kiseonika u tečnom antimonu, bizmutu i legurama bizmuta i antimonan određen je eksperimentima kulometrijske titracije koji su izvođeni u temperaturnom rasponu od 985 do 1185 K. Difuzivnost kod čistih metala (u cm^2/s) je:

$$D_O^{Bi} = (9.04 \pm 1.82) \cdot 10^{-3} \exp\left(\frac{-49115 \pm 1809}{RT}\right)$$

$$D_O^{Sb} = (2.87 \pm 0.22) \cdot 10^{-4} \exp\left(\frac{-16720 \pm 677}{RT}\right)$$

Izračunata je standardna slobodna energija rastvora kiseonika u tečnom antimonu, bizmutu, i legurama antimona i bizmuta prema reakciji ½ O_2 (g) = O (beskonačno razblaživanje). Koeficijent aktivnosti kiseonika $\gamma^0_{O(Bi,\ Sb\ or\ Bi\text{-}Sb)}$ izračunat je na temperaturi od 1085 K kao funkcija sastava legure. Pokazano je da je Vagnerov model sa jednim promenljivim parametrom h dao zadovoljavajući opis eksperimentalnih podataka.

Ključne reči: *Metod kulometrijske titracije; Koeficijent aktivnosti kiseonika; Difuzivnost kiseonika; Bi-Sb legure*